

Superplasticity: A Review

G. J. DAVIES, J. W. EDINGTON, C. P. CUTLER, K. A. PADMANABHAN
Department of Metallurgy, University of Cambridge, Pembroke Street, Cambridge

1. Introduction

The phenomenon of superplasticity wherein specimens deformed in tension at low stresses exhibit essentially neck-free elongations of many hundreds of per cent, was first reported* by Jenkins [1]. Subsequently, Bochvar, Presnyakov and co-workers (see Underwood [4]) revived interest in the subject and following the work of Backofen *et al* [5], a considerable volume of literature describing superplastic alloys has appeared.

Superplastic materials can broadly be divided into two groups:

(1) those in which a characteristic structural condition exists, e.g. a stable ultra-fine grain size, and

(2) those for which special testing conditions are necessary, e.g. temperature cycling under a small applied stress.

In both groups the applied stress for superplastic deformation is markedly dependent on the strain rate. This dependence seems to be evaluated best in terms of the strain rate sensitivity index, m ($= \partial \log \sigma / \partial \log \dot{\epsilon}$) in the relationship (Backofen *et al* [5]),

$$\sigma = K \dot{\epsilon}^m \quad (1)$$

where σ is the applied stress, $\dot{\epsilon}$ is the strain rate and K is a constant for given testing conditions. It should be noted that the constant K and the strain-rate sensitivity index, m , are both dependent on test parameters such as temperature and grain size. For Newtonian-viscous solids ($m = 1$) elongation in tension should be uniform and independent of irregularities in cross-section. Although m is not normally greater than about 0.8 for superplastic materials, it is expected that the deformation will be relatively stable in a tensile test for $m \gtrsim 0.5$. In practice this seems to be the case since for superplastic materials increased resistance to necking and high elongations are apparent for m greater than about 0.3. However, the elongation during superplastic

flow is not entirely neck-free, but instead a series of rather diffuse necks develops. The relationship between the strain-rate sensitivity and the stability of plastic flow is reviewed in detail in section 2.

The group (1) materials which exhibit "structural" superplasticity with m of the order of 0.3 to 0.8 are considered in section 3. Firstly the main experimental evidence is reviewed (section 3.1) and subsequently a detailed examination is made of the numerous mechanisms proposed to account for structural superplasticity (section 3.2).

Superplasticity in the group (2) materials is observed with $m \sim 1$. Less information is available for these materials and the data are reviewed in section 4.1, while in section 4.2, the theoretical mechanisms for "environmental" superplasticity are examined.

Finally, in section 5, attention is given to the application of superplasticity in practice, both for the manufacture of components and as a means of producing microstructures which have superior in-service properties.

2. The Relationship between Strain-Rate Sensitivity and the Stability of Plastic Flow

During tensile deformation at temperatures less than about $0.4 T_m$ the plastic flow of metals is stabilised by strain-hardening effects. If the material being deformed obeys a true stress-true strain law of the type (see for instance [6]),

$$\sigma = C \epsilon^n \quad (2)$$

where C , the strength coefficient and n , the strain-hardening exponent, are constants, the true strain at which plastic instability (necking) occurs can be shown both theoretically and experimentally [7], to be,

$$\epsilon_{\text{necking}} = n$$

n usually lies within the range 0.1 to 0.3.

*Superplastic behaviour in torsion was first reported by Saveur [2] Pearson [3] first presented detailed observations of tensile superplasticity.

At elevated temperatures the rate of strain-hardening (and therefore, n) decreases, but nevertheless extensive plastic deformation occurs without necking. In this case plastic stability results from an enhanced strain-rate sensitivity [8, 9]. The stability of plastic deformation when both strain-hardening and strain-rate effects need to be considered has been examined by Rossard [10], Hart [11] and Campbell [12] with similar results. Assuming a generalised flow stress law,

$$\sigma = K' \epsilon^n \dot{\epsilon}^m \quad (3)$$

where K' is a constant embracing C and K , it was shown that deformation is stable provided

$$\frac{n}{\epsilon} + m \geq 1$$

This criterion is in agreement with that cited above for materials which show no rate dependence of strain-hardening. It is also in agreement with the criterion for viscous materials ($n = 0$) which are resistant to necking for $m \geq 1$ [13]. Furthermore, if we consider the case where n is small and equation 3 reduces to equation 1, then the rate at which the strain gradients increase is expected to be low for $m \gtrsim 0.5$ [10, 12] even though a state of plastic instability exists. This is consistent with the formation of a series of diffuse necks.

3. Structural Superplasticity in Metals

3.1. Experimental Data

3.1.1. Mechanical Properties

Structural superplasticity has been observed in a large range of two-phase alloys, many of which are based on eutectic or eutectoid compositions. In addition, it has been demonstrated that relatively pure metals can also behave superplastically under special testing conditions. Appendix 1 contains a complete list of materials known to show structural superplasticity or to exhibit anomalous ductility.

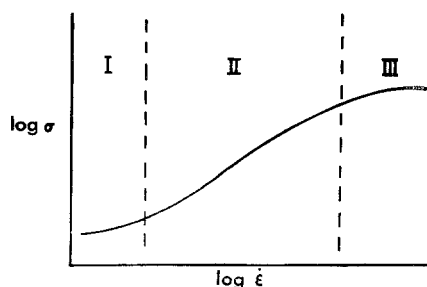


Figure 1 The relationship between stress and strain-rate (schematic).

Most superplastic materials exhibit a sigmoidal variation of $\ln \sigma$ with $\ln \dot{\epsilon}$ (fig. 1). The region of maximum strain-rate sensitivity (region II) with slope $m \gtrsim 0.3$ delineates the strain rate range over which superplasticity occurs. Both the low and high regions exhibit values of $m \sim 0.1$ and correspond to conventional plasticity. Many materials, e.g. alloys of lead-tin [14, 16], tin-bismuth [21], aluminium-copper [53, 54] and copper-zinc [56] show all three regions. In contrast, some materials, zinc-aluminium [34], nickel-base [59], and titanium-base [70] alloys only show regions II and III.

There is very little experimental data available for region I. However, Holt [37] has reported that there is less grain boundary sliding than in region II. In addition, striations at transverse grain boundaries have been reported [18] and there is some evidence for grain elongation [53]. The implication of these results is that Nabarro-Herring creep may be playing an increasingly important role in deformation.

Studies of materials deformed in region III show that slip lines can be observed on the surface [18, 37] and that a high density of dislocations is visible within the grains [44, 59, 73]. In addition, some grain boundary sliding is observed [53]. It is, therefore, generally agreed that the deformation in this region involves slip and recovery creep.

A large number of experiments have been carried out on the superplastic region II, but they have not produced data which define a unique rate-controlling mechanism. Nevertheless, it has been clearly demonstrated that three important criteria must be satisfied if superplastic behaviour is to occur. These are:

(1) The material must have a fine ($< 10 \mu\text{m}$ diameter) equiaxed grain size which remains stable at the temperature of deformation. The simplest way of obtaining the required stable grain structure is by producing a two-phase mixture in which the phases are present in approximately equal proportions. In general, such alloys are of eutectic or eutectoid composition. The as-cast material is heavily hot worked to produce an intimate mixture of the two phases such that both phases have fine grain sizes. In some cases, spinodal decomposition also produces the correct structure [41] and two-phase mixtures in which one phase pins the grain boundaries of the other are also effective in stabilising the grain size so as to produce superplasticity [26-30].

If one of the phases has a large grain size [53]

(e.g. an annealed eutectic alloy), if grain growth occurs during testing [16, 59, 60], or if the grains are not equiaxed [14, 21, 41, 53] the ability to show superplasticity is lost.

(2) The strain rate sensitivity index, m , of the material should be high, i.e. $m > 0.3$ compared with values ~ 0.1 for conventional deformation. The behaviour occurs in region II of fig. 1 and it has been found that the value of m depends on grain size, temperature of deformation and strain rate. In general, m increases with decreasing grain size (fig. 2) or increasing temperature (fig. 3), but goes through a maximum with increasing strain rate (fig. 3). Maximum elongations are

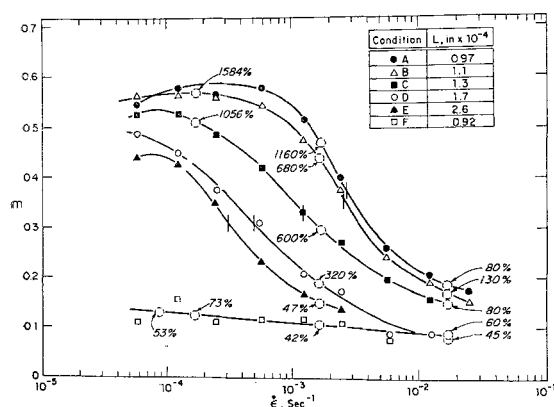


Figure 2 The dependence of the strain-rate sensitivity index on strain rate of lead-tin eutectic specimens with different grain sizes (L = grain size or metallographic mean free path) (Avery and Backofen [14]).

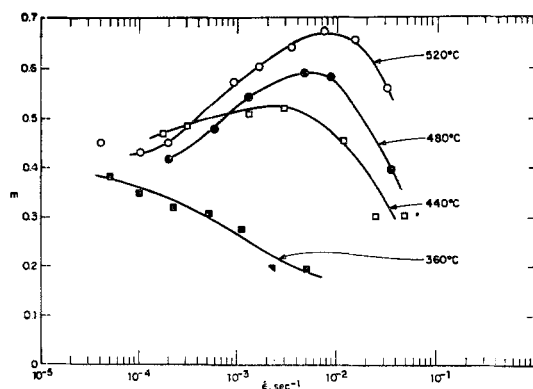


Figure 3 The dependence of the strain-rate sensitivity index on strain rate at different temperatures for aluminium-copper eutectic specimens (Holt and Backofen [53]).

frequently found under conditions of maximum m and it has been pointed out [74] that there is a general relationship between the value of m and the elongation to fracture. However, there is considerable scatter in the results and detailed interpretation of the relationship is not possible at present.

There is some indication that the diffusion rates in both phases of duplex alloys should be similar at the deformation temperature if superplasticity is to take place. For example, the aluminium-copper eutectic alloy can be made superplastic, but the aluminium-silicon eutectic cannot. In the latter alloy, values of $m = 0.4$ have been reported but maximum elongations

TABLE I Reported values of the activation energy for superplastic deformation (region II, fig. 1) together with measured values for diffusional processes

Material	Activation energy for superplastic deformation K.Cals/mol.	References	Activation energy for self-diffusion [76] K.Cals/mol.	Activation energy for grain-boundary diffusion K.Cals/mol.	References
Sn-Pb eutectic	11.5	16	25 (Sn) 25 (Pb)	9.5 (Sn) 15.7 (Pb)	77 78
Sn-5% Bi	9.6	115	25 (Sn)	9.5 (Sn)	77
Pb-5% Cd	9.6	22	25 (Pb)	15.7 (Pb)	78
Cd-5% Pb	10	79	19 (Cd)	9.5 (Cd)	79
Zn-0.2% Al	10	80	21.8-25 (Zn) 34 (Al)	14 (Zn)	81
Zn-Al eutectoid	14.5	44	21.8-25 (Zn) 34 (Al)	14 (Zn)	81
Fe-Ni-Cr	60	59	60 (Fe) 69.8 (Ni)		
Ti-alloys	50-65	70	29.3 28.5-54 [82-84]		

are less than 100% [104]. However, the situation is complicated by grain growth during the test and the above interpretation of the data is not unique.

In alloys satisfying the above three criteria, it has been found that an activation energy Q for the deformation process can be determined from the experimental relationship,

$$\dot{\epsilon}_{\sigma,L} \propto \exp - \frac{Q}{kT} \quad (4)$$

where k is Boltzmann's constant and $\dot{\epsilon}$ is the strain rate. Table I contains a summary of the values of activation energy reported for superplastic deformation in a number of materials.

The activation energy is largely independent of particle size, but its meaning is not at all clear since it can be seen from Table I to be of the order of magnitude of the activation energy for volume diffusion in Fe-Ni-Cr and Ti alloys, and of the activation energy for grain boundary diffusion for Sn, Pb, Zn alloys. Nonetheless, it is apparent that diffusional processes are of considerable importance in superplastic flow. This view is reinforced by the recent observation [17] that alloying elements which increased atomic mobility also enhanced superplastic behaviour.

The strain rate corresponding to a given flow stress and temperature has been shown to vary with grain size, L as:

$$\dot{\epsilon} \propto \frac{1}{L^a} \quad (5)$$

where the exponent a has been given as 2 [14, 44, 53, 54] and as 3 [21, 39]. In these circumstances, it would seem justifiable to accept the views of Jones and Johnson [85] and Packer and Sherby [39] that the exponent can only be considered to lie within the above values as limits.

A somewhat similar variation in results has been reported for the dependence of flow stress on grain size at constant strain rate and temperature. In this case

$$\sigma \propto L^b \quad (6)$$

where b has been reported as lying in the range 0.7 to 1.2 [39, 42, 53, 60, 70].

Combining equations 4, 5 and 6 gives the general dependence of strain rate during superplastic deformation on stress level, grain size and temperature as

$$\dot{\epsilon} = \text{constant} \cdot \frac{\sigma^n}{L^a} \exp \left(- \frac{Q}{kT} \right) \quad (7)$$

where n is a/b and lies in the range 1.6 to 4.2.

Comparison of this equation with the equation 1 indicates that $n \sim 1/m$ with m the strain-rate sensitivity index and lies in the range 0.3 to 0.7.

3.1.2. Metallography

Metallographic observations during superplastic flow are broadly in agreement and it has been shown that the grain structure remains essentially equiaxed, with little growth during deformation under optimal conditions. Detailed metallographic studies [54] of the aluminium-copper eutectic showed that sintering of CuAl_2 particles occurred during superplastic deformation. Similar effects for lead particles in the lead-tin eutectic alloy have also been observed [19]. Optical metallography has also demonstrated that significant amounts of grain boundary sliding occur.

The surface of superplastically deformed alloys has been studied by replica techniques and by scanning electron microscopy. There was no evidence of microscopic slip, but clear evidence of grain boundary sliding [44]. Very recently, *in situ* scanning electron microscopy studies [86] of superplastically deforming lead-tin eutectic alloy have shown that grains tend to rotate in clumps by grain boundary sliding around the boundary of the clumps.

Transmission electron microscopy studies of superplastically deformed ($m \sim$ maximum) eutectoid aluminium-zinc [41] and nickel-base alloys [59] showed that the grains were almost entirely free of dislocations. Such investigations also demonstrated that the grain boundaries were smooth, free of large ledges and contained no absorbed dislocations like those seen by Gleiter [87] in nickel-base alloys.

However, considerable relaxation of any dislocation configurations which might be present during testing is likely, after the load is removed and the specimen is cooled to room temperature, before being electro-thinned to make a thin foil suitable for transmission electron microscopy. Consequently the almost complete absence of dislocations in thin foils is not definitive evidence for their absence during the test. Further it has been shown [75] that the precipitation of semi-coherent α' on (111) planes of the aluminium-rich phase of the zinc-aluminium eutectoid alloy does not affect the superplastic properties of the alloy and that subsequently, no dislocations are visible tangled up with the precipitates. This implies that macroscopic slip had not occurred in this phase. On the other hand, superplastic deform-

ation produces precipitate-free zones near grain boundaries and thus it can be concluded that grain boundary movement occurs.

Fike and Rack [45] have also presented direct evidence for grain boundary sliding by deforming a thin foil of the zinc-aluminum eutectoid alloy at 250°C, at an unspecified strain rate. However, the geometry of the specimen, and the complex stress field, together with the observed cracking of the specimen make this observation of doubtful significance in relation to bulk superplastic deformation.

In summary, there is considerable metallographic evidence for the importance of grain boundary sliding in superplastic deformation, but there is no evidence for significant slip. However, there remains the evidence that rod specimens of the zinc-aluminium eutectic alloy become elliptical in cross-section during superplastic deformation [33]. This could be interpreted in terms of a slip process although structural inhomogenities could also produce this effect.

Several workers have used X-ray texture measurements to study superplasticity. Back reflection Laue measurements [39] failed to detect texture in either undeformed or superplastically deformed zinc-aluminium eutectoid alloy. However, more accurate conventional texture measurements [33] performed on sheet specimens of the eutectic zinc-aluminium alloy demonstrated that the texture in the zinc-rich matrix was reduced and changed by superplastic deformation. In the light of the concomitant shape change of the specimen during deformation, this result was interpreted in terms of combined crystallographic slip and grain boundary migration. Similar texture changes [27-30] were observed for the zinc-rich phase of the zinc-0.4% aluminium alloy, but differences in detail occurred depending on the angle between the rolling and tensile directions. In recent experiments [19] the variation of texture with strain for a range of values of m has been studied in the lead-tin eutectic alloy. The texture of both lead and tin rich phases has been measured in strip specimens produced by rolling cast material at room temperature. It has been shown that for $m = 0.3$ to 0.7 the texture in the lead is completely removed after 200% strain, but the texture in the tin is weakened and changed up to the maximum (500%) strain investigated. For the lead-rich phase, the angle between the rolling direction and the tensile axis influences the rate

of change of texture, but not the final result. However, for the tin-rich phase both the rate of change of texture and the details of the final texture depend on the angle between the tensile axis and rolling direction.

All texture measurements described above [19, 27-30, 33] have been confined to the central 70° of the stereogram. Consequently, quantitative interpretation of the data is not possible although the general importance of grain boundary sliding, implied by many of the metallographic studies, is consistent with the texture measurements. The latter results [19] on the lead-tin eutectic imply, however, that the amount of sliding on lead/lead, lead/tin and tin/tin boundaries is different.

3.2. Proposed Mechanisms

A number of mechanisms have been proposed to account for structural superplasticity.

(a) The earliest theories, those of Bochvar and Presnyakov (see Underwood [4]) involved solution-precipitation fluctuations or a breakdown of an initially metastable state. As the class of alloys which exhibited superplasticity was enlarged these theories were shown to be inadequate [38].

Other theories are:

(b) Diffusion-creep, either through the bulk of the grains (Nabarro-Herring) [14] or along grain boundaries [85]. However, it has been shown by Alden [21] and Hayden *et al* [59] that the calculated values of strain rates based on these theories are too small, often by several orders of magnitude. Furthermore, Nabarro-Herring creep would predict the formation of elongated grains, and the maintenance of any crystallographic texture existing prior to deformation. This is in conflict with the experimental observations that the grain structure remains equiaxed during deformation under optimal conditions, and that in general, texture is destroyed by superplastic deformation.

On the other hand, there is evidence that mass transfer along boundaries does occur during superplastic deformation in some alloys [50, 51]. (c) Dislocation climb in which control is exerted by dislocation motion in the bulk of the grains [59, 60] or along grain boundaries. These theories have been closely examined by Chaudhari [38] and Stowell [73] who established that mechanisms involving volume diffusion predicted strain rates that are far too small. Alden [88], as a result of a detailed study, concluded

that the dislocation climb theories are unsatisfactory for superplasticity. The position is not completely clear, however, particularly when the grain boundaries are considered since dislocation climb in the boundaries could well be a concomitant part of grain boundary sliding.

(d) Chaudhari [38], after examining dislocation climb mechanisms, proposed a theory in which superplastic flow was controlled by the diffusion-regulated glide of dislocations. The absence of dislocations and cells in the grains after superplastic deformation makes a justification of this model difficult. Added difficulties arise from the observations that flow stresses are low, that no strain hardening occurs and that the onset of slip leads to a loss of superplasticity.

On the other hand it has been reported [33] that after superplastic deformation originally cylindrical specimens became elliptical and that this could only be accounted for if some crystallographic slip occurred.

(e) The model of Johnson *et al* [33, 43] involved a combination of intergranular deformation (perhaps by grain boundary sliding) followed by recrystallisation. Three observations cast doubt on this model. Firstly, there is no periodic fluctuation in the flow stress during superplastic flow, as would be expected if repeated recrystallisation occurred [21]. Secondly, in high temperature creep under thermal and mechanical conditions similar to those required for superplastic deformation *no* recrystallisation takes place [89], and thirdly no recrystallisation is seen during direct observation of superplastic flow [45].

(f) By far the most viable models are those which involve grain-boundary sliding in association with some accommodation mechanism to achieve compatibility at grain boundaries [53]. The different models are;

- (i) a combination of grain boundary sliding and diffusion creep [14, 18, 53, 54, 89];
- (ii) a combination of grain-boundary sliding and grain-boundary migration [37];
- (iii) a multiple combination of grain-boundary sliding, grain-boundary migration and localised dislocation motion by glide and/or climb [21, 22, 52].

The cases for the individual models are equivocal. Nevertheless the bulk of the evidence suggests that the grain boundaries are the significant structural elements. Large amounts of grain-boundary sliding have been observed experimentally both directly [44, 45] and indirectly

as a result of the study of grain-boundary displacements [21, 37, 52]. Furthermore, direct evidence has been provided [50, 51] that there is considerable diffusion in the boundaries during superplastic deformation and Morrison [17] has shown that alloying elements which enhance diffusion also enhance superplastic behaviour. On the other hand, it has been pointed out that in the two-phase structures where the phases are structurally and chemically dissimilar, sliding cannot be accommodated without large redistribution of solute [33, 43]. However, Alden and Schadler [36] found that *interphase* boundaries and *intercrystalline* boundaries are similar in their contribution to superplasticity. These latter two observations raised difficulties in the acceptance of the different models mentioned above since they imply the existence of long range diffusion across phase boundaries.

The main difficulty in models involving grain-boundary sliding is the requirement that sliding must take place as a unit process, thus requiring repeated accommodation.

In the present case, it is felt that the important contribution of displacements in the grain-boundary region cannot be neglected and that the apparent "viscosity" of the grain boundaries [22, 42, 53] should be investigated further. In doing so, the evidence [36, 42] that the boundaries are regions both of poor misfit and abnormally high vacancy concentration under conditions of superplastic flow should be taken into account.

4. Environmental Superplasticity in Metals

4.1. Experimental Data

It has been found that a small number of polycrystalline materials become "spontaneously plastic" and change shape, independent of applied stress, under well-defined environmental conditions. The most common conditions under which this occurs are:

- (a) during temperature cycling through a phase change [90-92];
- (b) during temperature cycling of a thermally anisotropic material [93];
- (c) during neutron irradiation [94].

Superplastic behaviour is generally observed in these materials when a small stress is applied in conjunction with the above conditions.

The materials for which environmental superplasticity has been shown to occur are usually subjected to condition (a). Experimental data

referring to these materials are given in Appendix 2, together with some values for the maximum observed strains per temperature cycle. In most cases the total strain per temperature cycle is small, 10^{-2} , but depends on the transformation and increases with increasing applied stress (see fig. 4). A linear relationship between applied stress σ , and external strain rate, $\dot{\epsilon}$, has been found in many materials [95, 96, 102].

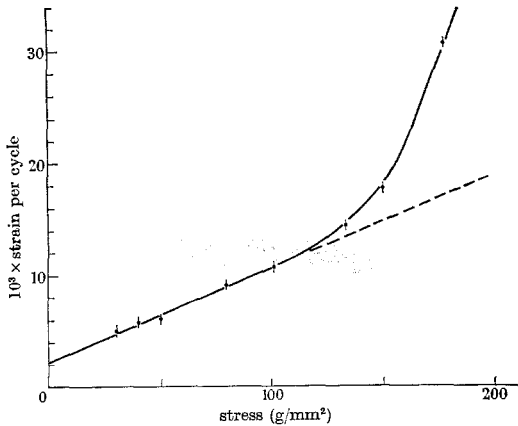


Figure 4 Strain per complete two-way cycle plotted against applied stress for the α/β transformation in titanium at 882°C (Greenwood and Johnson [92]).

However, above a critical external stress this linear relationship often breaks down [95, 102].

Although a large number of materials exhibit a shape change after undergoing a phase transformation, only one case has been reported for specimens cycled to failure. Oelschlagel and Weiss [90] produced large extensions $> 500\%$ in iron by repeated cycling (~ 200 times) through the $\alpha + \text{Fe}_3\text{C}/\gamma$ region (fig. 5). Research in this area could well be devoted to some martensitic and bainitic transformations [97, 98] which produce strains on transformation of up to 4% in steels, but have not been investigated in terms of strain to fracture.

It is also important to note that single transformations have been reported to enhance the ductility of certain steels [99]. For example, metastable austenitic stainless steels exhibit high elongations ($\sim 100\%$) when deformed at temperatures at which martensite is formed during straining, and similar effects have been found for the intermetallic compound NiTi [100, 101].

Superplasticity produced by temperature cycling of thermally anisotropic materials has not received much attention. There is, however, one

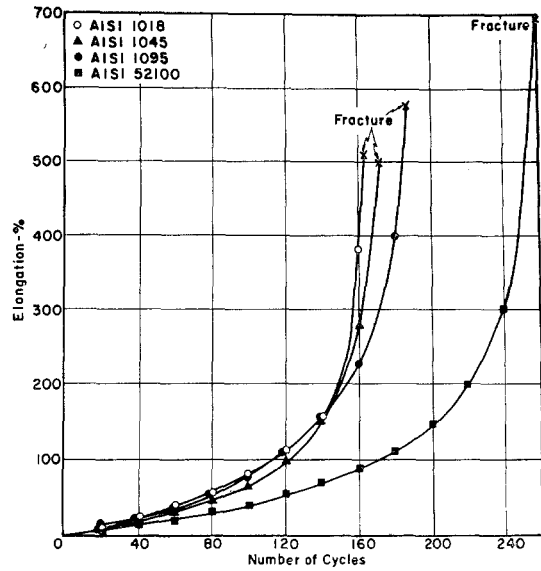


Figure 5 Deformation due to temperature cycling between 1000 and 1500°F versus number of cycles for four steels. Constant load $\sigma_0 = 2500$ psi (Oelschlagel and Weiss [90]).

well-documented case of α -uranium [93]. If this material is thermally cycled between 400 and 600°C , elongations of 170% are produced in polycrystalline material under a load of 115 kg mm^{-2} and total extensions of $\sim 300\%$ have been achieved. These values compare with an elongation to fracture of conventionally tested material of 55% at 600°C .

Finally, superplastic behaviour under a neutron irradiation environment has been reported for α -uranium [94]. Under stresses of 0.01 times the yield stress Y and irradiation at 100°C the material exhibits a steady strain rate of $3 \times 10^{-11}\text{ sec}^{-1}$ and approximately obeys a pseudo-creep law of the form

$$\dot{\epsilon} \propto \frac{\sigma}{Y} \dot{\epsilon}_g,$$

where $\dot{\epsilon}_g$ is the swelling rate of individual grains. This equation is equivalent to $m = 0.8$, but large elongations have not been demonstrated because of the low strain rate involved.

4.2. Proposed Mechanisms

The most surprising feature of environmental superplasticity is the very low applied stress which is necessary to produce deformation. Cottrell [102] has pointed out that this arises because the yield strength of the material has

been overcome by intergranular stresses arising from the phase transformation, thermal anisotropy, etc. The applied stress simply perturbs and directs the existing motion in the material.

Several deformation mechanisms have been proposed to account for the details of superplasticity associated with phase transformation: (i) loss of cohesion between atoms in the interface between phases as they move into new positions [4];

(ii) recovery creep enhanced by the abundance of point defects created during volume change which takes place on the transformation austenite to ferrite and vice versa [103];

(iii) the interaction and absorption of dislocation pile-ups in the austenite/ferrite interface [97];

(iv) grain boundary segregation of carbon in ferrite which locally promotes transformation to austenite at the grain boundaries [105, 106].

Although these models provide a qualitative description of superplasticity there is little direct evidence for their occurrence, such as might be produced by transmission electron microscopy studies.

The most satisfactory approach to describing phase transformation superplasticity is that due to Greenwood and Johnson [92]. These workers do not specify the deformation mode and only assume that the plastic deformation is restricted to the weaker phase present during temperature cycling.

The total strain in a thermal cycle is then the sum of the transformation strain, the superimposed normal creep strain in the weaker phase and the fractional change in length corresponding to the volume change associated with the transformation. The analysis leads to a linear relation between stress and strain.

5. Applications of Superplasticity

The utilisation of structural superplasticity for forming artefacts has two main advantages. Firstly, large strains can be obtained without the fear of localised necking and secondly, the stresses under which superplastic deformation takes place are low. The main disadvantage is that the strain rates are also low and are in most cases considerably smaller than those employed in most conventional forming operations.

A convincing demonstration of the potential of these superplastic materials was given by Backofen, Turner, and Avery [5] for sheet-bulging. Subsequently, Fields [40] demonstrated the vacuum thermoforming of the zinc-alumin-

ium eutectoid. He was able to show both that large draw ratios could be produced and that the material was capable of preserving the detail to a very high degree (fig. 6).

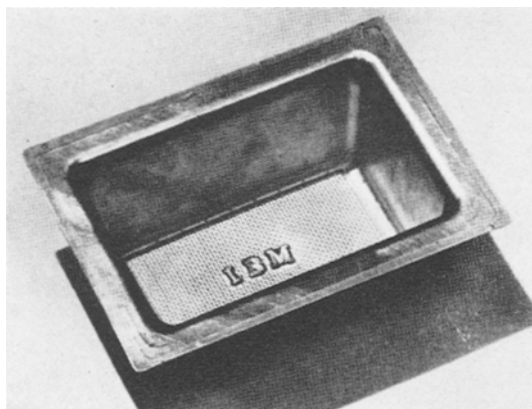


Figure 6 Vacuum-formed part with bottom surface developed over wire mesh and plastic characters (Fields [40]).

In both cases the behaviour of the superplastic material was very similar to that of polymer materials and a number of workers (see, for instance, Johnson [107]) emphasised the possibility of adapting established techniques for forming polymers to the forming of superplastic metals. The techniques considered included vacuum forming, drape forming, bottle blowing, etc.

Recently, Al-Naib and Duncan [108] presented a most comprehensive study of the forming of superplastic metals. They used the superplastic lead-tin eutectic alloy and illustrated a variety of pressure-forming techniques. The results of this study showed quite clearly that within limits superplastic behaviour can be utilised in forming in many different ways.

The larger-scale exploitation of superplasticity by industry, particularly the motor industry, has been discussed by Hundy [109]. It was pointed out that the pattern of costs was very different from that encountered in conventional sheet-metal forming. However, superplastic behaviour might be used industrially if complex welded assemblies could be replaced by a single superplastically pressed component.

Before a commercially viable application of superplastic forming can be envisaged, a means of carefully assessing forming operations is necessary. A number of theoretical analyses of

forming operations using materials which obey equation 1 have been presented [110-112] and experimentally verified. These results are important if widespread application is to be achieved, and process design is to be effective. However, further equations must be developed which relate all the process variables in such a way as to allow the calculation of loads, etc. in addition to providing data on which an optimisation of conditions can be based. A numerical method for deriving such equations has been given by Padmanabhan and Davies [113].

Exploitation of environmental superplasticity has received less attention, although Johnson [107] has proposed a technique of die-less drawing which should be applicable to this type of deformation.

One aspect of the use of superplastic metals was that considered by Hayden *et al* [59] who observed that the microstructural condition which favoured superplastic behaviour could also give rise to an improvement in a number of the properties desirable in subsequent service. There is a need for further exploration of the properties of materials *after* superplastic deformation. For instance, although some apprehension has been expressed about the creep resistance of the as-formed metal the results of Naziri and Pearce [114] are most encouraging. They showed that the addition of small amounts of copper to the zinc-aluminium eutectoid had no effect on the superplastic behaviour or the formability but led to markedly improved creep strength.

Acknowledgement

The authors would like to thank the Ministry of Technology for providing support for the research programme during which this review was prepared.

References

1. C. H. M. JENKINS, *J. Inst. Metals* **40** (1928) 21.
2. A. SAVEUR, *Iron Age* **113** (1924) 581.
3. C. E. PEARSON, *J. Inst. Metals* **54** (1934) 111.
4. E. E. UNDERWOOD, *J. Metals* **14** (1962) 914.
5. W. A. BACKOFEN, I. R. TURNER, and D. H. AVERY, *Trans. ASM* **57** (1964) 980.
6. G. E. DIETER, "Mechanical Metallurgy" (McGraw-Hill, New York, 1961), p. 55.
7. J. D. LUBAHN, *Trans. ASME* (May 1946), p. 277.
8. A. NADAI and M. J. MANJOINE, *J. Appl. Mech.* **8** (1941) A77.
9. D. S. FIELDS, JR. and W. A. BACKOFEN, *Trans. ASM* **51** (1959) 946.
10. C. ROSSARD, *Rev. Met.* **63** (1966) 225.
11. E. W. HART, *Acta Metallurgica* **15** (1967) 351.
12. J. D. CAMPBELL, *J. Mech. Phys. Sol.* **15** (1967) 359.
13. E. OROWAN, *Reports Progr. Physics* **12** (1948-49) 185.
14. D. H. AVERY and W. A. BACKOFEN, *Trans. ASM* **58** (1965) 551.
15. P. J. MARTIN and W. A. BACKOFEN, *ibid* **60** (1967) 352.
16. H. E. CLINE and T. H. ALDEN, *Trans. Met. Soc. AIME* **239** (1967) 710.
17. W. B. MORRISON, *ibid* **242** (1968) 2221.
18. S. W. ZEHR and W. A. BACKOFEN, *Trans. ASM* **61** (1968) 300.
19. C. P. CUTLER and J. W. EDINGTON, to be published.
20. T. H. ALDEN, *Trans. Met. Soc. AIME* **236** (1966) 1633.
21. *Idem*, *Acta Metallurgica* **15** (1967) 469.
22. *Idem*, *Trans. ASM* **61** (1968) 559.
23. R. CHADWICK, *J. Inst. Metals* **54** (1934) 131.
24. D. WILLIAMS, H. NAZIRI, and R. PEARCE, College of Aeronautics, Cranfield, Report No. 137 (1967).
25. C. H. MATHEWSON, C. S. TREWIN, and W. H. FINKELDEY, *Trans. AIME* **64** (1920) 305.
26. R. C. COOK and N. R. RISEBROUGH, *Scripta Met.* **2** (1968) 487.
27. H. NAZIRI and R. PEARCE, *J. Inst. Metals* **97** (1969) 326.
28. *Idem*, *Scripta Met.* **3** (1969) 807.
29. *Idem*, *ibid* **3** (1969) 811.
30. *Idem*, *J. Inst. Metals* **98** (1970) 71.
31. D. TROMANS and J. A. LUND, *Trans. ASM* **59** (1966) 672.
32. W. H. MCCARTHY, J. C. SHYNE, and O. D. SHERBY, *Nature* **208** (1965) 579.
33. C. M. PACKER, R. H. JOHNSON, and O. D. SHERBY, *Trans. Met. Soc. AIME* **242** (1968) 2485.
34. A. A. BOCHVAR and Z. A. SVIDERSKAYA, see UNDERWOOD [4].
35. A. A. PRESNYAKOV and V. V. CHERVYAKOVA, see UNDERWOOD [4].
36. T. H. ALDEN and H. W. SCHADLER, *Trans. Met. Soc. AIME* **242** (1968) 825.
37. D. L. HOLT, *ibid* **242** (1968) 25.
38. P. CHAUDHARI, *Acta Metallurgica* **15** (1967) 1777.
39. C. M. PACKER and O. D. SHERBY, *Trans. ASM* **60** (1967) 21.
40. D. S. FIELDS JR., *IBM J. Res. Dev.* **9** (1965) 134, see also *US Pat. No.* 3,340,101 and *UK Pat. No.* 1,120,007.
41. K. NUTTALL and R. B. NICHOLSON, *Phil. Mag.* **17** (1968) 1087.
42. R. KOSSOWSKY and J. H. BECHTOLD, *Trans. Met. Soc. AIME* **242** (1968) 716.
43. R. H. JOHNSON, C. M. PACKER, L. ANDERSON, and O. D. SHERBY, *Phil. Mag.* **18** (1968) 1309.

44. A. BALL and M. M. HUTCHISON, *Metal Sci. J.* **3** (1969) 1.
45. K. D. FIKE and H. J. RACK, *Trans. ASM* **62** (1969) 537.
46. D. L. HOLT, *Trans. Met. Soc. AIME* **242** (1968) 740.
47. *Idem*, *Trans. ASM* **60** (1967) 564.
48. J. A. CHAPMAN and D. V. WILSON, *J. Inst. Metals* **91** (1962) 39.
49. P. GREENFIELD and W. VICKERS, *J. Nuclear Materials* **22** (1967) 77.
50. W. A. BACKOFEN, G. S. MURTY, and S. W. ZEHR, *Trans. Met. Soc. AIME* **242** (1968) 329.
51. A. KARIM, D. L. HOLT, and W. A. BACKOFEN, *ibid* **245** (1969) 1131.
52. D. LEE, *Acta Metallurgica* **17** (1969) 1057.
53. D. L. HOLT and W. A. BACKOFEN, *Trans. ASM* **59** (1966) 755.
54. M. J. STOWELL, J. L. ROBERTSON, and B. M. WATTS, *Metal Sci. J.* **3** (1969) 41.
55. A. A. PRESNYAKOV and G. V. STARIKOVA, see UNDERWOOD [4].
56. D. M. R. TAPLIN, G. L. DUNLOP, S. SAGAT, and R. H. JOHNSON, University of Waterloo, Ontario, Solid Mechanics Division, Report No. 29 (1970).
57. H. E. CLINE and D. LEE, *Acta Metallurgica* **18** (1970) 315.
58. S. FLOREEN, *Scripta Met.* **1** (1967) 19.
59. H. W. HAYDEN, R. C. GIBSON, H. F. MERRICK, and J. H. BROPHY, *Trans. ASM* **60** (1967) 3.
60. H. W. HAYDEN and J. H. BROPHY, *ibid* **61** (1968) 542.
61. R. J. LINDINGER, R. C. GIBSON, and J. H. BROPHY, *ibid* **62** (1969) 230.
62. D. WEINSTEIN, *Trans. Met. Soc. AIME* **245** (1969) 2041.
63. R. C. GIBSON, H. W. HAYDEN, and J. H. BROPHY, *Trans. ASM* **61** (1968) 85.
64. A. R. MARDER, *Trans. Met. Soc. AIME* **245** (1969) 1337.
65. A. GOLDBERG, *JISI* **204** (1966) 268.
66. H. W. SCHADLER, *Trans. Met. Soc. AIME* **242** (1968) 1281.
67. W. B. MORRISON, *Trans. ASM* **61** (1968) 423.
68. J. R. STEPHENS and W. D. KLOPP, *Trans. Met. Soc. AIME* **236** (1966) 1637.
69. H. E. CLINE, *ibid* **239** (1967) 1906.
70. D. LEE and W. A. BACKOFEN, *ibid* **239** (1967) 1034.
71. J. E. LITTLE, G. FISCHER, and A. R. MARDER, *J. Metals* **17** (1965) 1055.
72. M. GARFINKLE, W. R. WITZKE, and W. D. KLOPP, *Trans. Met. Soc. AIME* **245** (1969) 303.
73. M. J. STOWELL, private communication.
74. D. A. WOODFORD, *Trans. ASM* **62** (1969) 291.
75. K. NUTTALL, private communication.
76. C. J. SMITHELLS, "Metals Reference Book", 4th Edition (Butterworths, London 1967), pp. 644, 645.
77. W. LANGE and D. BERGNER, *Phys. Stat. Sol.* **2** (1962) 1410.
78. B. OKKERSE, *Acta Metallurgica* **2** (1954) 551.
79. K. G. DONALDSON, see T. H. ALDEN [115].
80. R. C. COOKE, M.A.Sc. Thesis, University of British Columbia (1969).
81. E. S. WAJDA, *Acta Metallurgica* **2** (1954) 184.
82. C. M. LIBANATI and F. DYMENT, *ibid* **11** (1963) 1263.
83. J. F. MURDOCK, T. S. LUNDY, and E. E. STANSBURY, *ibid* **12** (1964) 1033.
84. S. P. MURARKA and R. P. AGARWALA, *ibid* **12** (1964) 1096.
85. R. B. JONES and R. H. JOHNSON, *Trans. ASM* **59** (1966) 356.
86. H. GLEITER, E. HORNBOKEN, and G. BARO, *Acta Metallurgica* **16** (1968) 1053.
87. H. GLEITER, *ibid* **16** (1968) 1167.
88. T. H. ALDEN, *ibid* **17** (1969) 1435.
89. R. C. GIFFKINS, *J. Inst. Metals* **95** (1967) 373.
90. D. OELSCHLÄGEL and V. WEISS, *Trans. ASM* **59** (1966) 143.
91. R. KOT and V. WEISS, *ibid* **60** (1967) 566.
92. G. W. GREENWOOD and R. H. JOHNSON, *Proc. Roy. Soc. A* **283** (1965) 403.
93. R. H. JOHNSON and E. C. SYKES, *Nature* **209** (1966) 192.
94. S. T. KONOBEEVSKY, N. F. PRAVDYU, and V. I. KUTAITSEVE, Proceedings of the International Conference on Peaceful Uses of Atomic Energy, **7** (1955) 433.
95. M. DE JONG and G. W. RATHENAU, *Acta Metallurgica* **7** (1959) 246.
96. D. A. ANKARA and D. R. F. WEST, *JISI* **205** (1967) 36.
97. L. F. PORTER and P. C. ROSENTHAL, *Acta Metallurgica* **7** (1959) 504.
98. R. H. BUSH and J. C. BOKROS, *ibid* **12** (1964) 102.
99. J. P. BRESSANELLI and A. MOSKOWITZ, *Trans. ASM* **59** (1966) 223.
100. W. J. BUEHLER and R. C. WILEY, *ibid* **55** (1962) 269.
101. *Idem*, *Mater. Design Eng.* **55** (1962) 82.
102. A. H. COTTRELL, "Mechanical Properties of Matter" (John Wiley, New York 1964) p. 338.
103. F. W. CLINARD and O. D. SHERBY, *Trans. Met. Soc. AIME* **233** (1965) 1975.
104. R. S. CHAPPELL and G. POLLARD, "Electron Microscopy 1968, Vol. 1" ed. D. S. Bocciarelli (Tipografia Poliglotta Vaticana, Rome 1968) p. 421.
105. M. G. LOZINSKY and I. S. SIMEONOVA, *Acta Metallurgica* **7** (1959) 709.
106. M. G. LOZINSKY, *ibid* **9** (1961) 689.
107. R. H. JOHNSON, *Design Engineering* (March 1969) p. 33.
108. T. Y. M. AL-NAIB and J. C. DUNCAN, *Internat. J. Mech. Sci.* **12** (1970) 463.
109. B. B. HUNDY, "Plasticity and Superplasticity". Institution of Metallurgists Review Course, Series 2, No. 3 (1969) p. 73.
110. F. JOVANE, *Internat. J. Mech. Sci.* **10** (1968) 403.

111. G. C. CORNFIELD and R. H. JOHNSON, *ibid* **12** (1970) 479.
112. D. L. HOLT, *ibid* **12** (1970) 491.
113. K. A. PADMANABHAN and G. J. DAVIES, *J. Mech. Phys. Sol.* **18** (1970) 261.
114. H. NAZIRI and R. PEARCE, *Internat. J. Mech. Sci.* **12** (1970) 513.
115. T. H. ALDEN, *J. Aust. Inst. Met.* **14** (1969) 207

Received 30 July and accepted 9 September 1970.

Appendix 1

Materials for which structural superplasticity (or anomalous ductility) has been reported. (All compositions in wt %).

Material	Reported maximum values		Temperature range °C	References
	<i>m</i>	% elongation		
Cd-Zn eutectic	—	400	20	1
Sn-Pb eutectic	0.6	700	20	1, 3, 14-19
Sn-2% Pb	0.5	—	20-80	16
Sn-81% Pb	0.5	—	20-80	16
Sn	0.5	—	20	16
Sn-Bi eutectic	0.2	1950	20	3
Sn-1% Bi	0.48	500	22	20
Sn-5% Bi	0.68	1000	20	21
Pb-5% Cd	0.35	—	20	22
Zn (commercial)	0.2	400	20-70	23-25, 27
Zn-0.2% Al	0.8	450	23	26
Zn-0.4% Al	0.43	550	20	28-30
Zn-ZnO ₂ particles	—	120	26	31
Zn-W particles	—	100	26	32
Zn-4.9% Al eutectic	0.5	300	200-360	33
Zn-22% Al eutectoid	0.7	1500	200-300	5, 34-46
Zn-40% Al	0.48	700	250	46, 47
Mg (commercial)	—	80	—	48
Mg-0.5% Zr	0.3	150	500	49
Mg-6% Zn-0.5% Zr	0.6	1000	270-310	50, 51
Mg-Al eutectic	0.8	2100	350-400	52
Al-Cu eutectic	0.9	500	440-520	19, 53-55
Cu-38% to 50% Zn	0.5	300	450-550	55, 56
Cu-10% Al-3% Fe	0.6	720	800	56
Cu-71.9% Ag	0.53	500	675	57
Ni	—	225	820	58
Ni-39% Cr-10% Fe-1.75% Ti-1% Al	0.5	1000	810-980	59-61
Fe-25% Cr-6% Ni	—	600	870-980	62, 63
Fe-C alloys	0.57	350	700	64, 65
Low alloy steels	0.65	400	800-900	66, 67
Cr-30% Co	—	160	1200	68
Co-10% Al	0.47	850	1200	69
Ti-5% Al-2.5% Sn	0.72	450	900-1100	70
Ti-4% Al-2.5% O	0.6	—	950-1050	70
Ti-6% Al-4% V	0.85	1000	800-1000	70, 71
Ti-0.3% impurity	0.8	—	900	70
Zircalloy	0.5	200	900	70
W-15% to 30% Re	0.46	200	2000	72

Appendix 2

Materials for which environmental superplasticity has been reported.

Material	Test Conditions		Transformation	Maximum elongation per cycle	References
	Stress g mm ⁻²	Temperature range °C			
Fe	550	910	$\alpha - \gamma$	1.6×10^{-2}	92
	800	870-930	$\alpha - \gamma$	1.5×10^{-2}	95
Fe-0.2 wt% C	1600	740-800	$\alpha - \gamma$	2.0×10^{-2}	95
Fe-0.4 wt% C	1800	540-816	$\alpha - \gamma$	4.0×10^{-3}	90
Fe-0.98 wt% C	1800	540-816	$\alpha - \gamma$	4.9×10^{-3}	90
Fe-1.07 wt% C	1800	540-816	$\alpha - \gamma$	3.3×10^{-3}	90
Fe-0.008 wt% N					
Co (spec. pure)	6500	417	$\epsilon - \alpha$	2.0×10^{-3}	92
Zr (iodide)	150	863	$\alpha - \beta$	1.9×10^{-2}	92
Ti (commercial)	180	882	$\alpha - \beta$	3.0×10^{-2}	92
U (commercial)	400	663	$\alpha - \beta$	1.0×10^{-2}	92
	125	770	$\beta - \gamma$	1.3×10^{-2}	92

Letter

Synthesis and Growth of Single Crystals of Gallium Nitride

Transparent single crystals of gallium nitride have been prepared in sizes ranging up to 1 mm thick and 5 mm in length. The growth occurs from a specially treated gallium nitride powder at temperatures of 1150 to 1200°C in a stream of dry NH₃ gas. Hot probe measurements indicate that the crystals are *N*-type and of very high conductivity. The growth takes place most likely by a sintering or surface diffusion process.

There is considerable interest in gallium nitride as a semiconducting compound because of its high bandgap, ~3.25 eV [1]. Light emission from gallium nitride devices can be in the visible or ultraviolet range of the spectrum. Gallium nitride has been made both *N*- and *P*-type [2, 3] and has a melting point estimated to be near 2000°C [4]. Most of the chemical, electrical and optical properties of gallium nitride have been obtained by the study of powdered or microcrystalline material. The method first described by Johnson *et al* [5], in which pure gallium is reacted with ammonia gas at 1000 to 1100°C has been used by most investigators to synthesise gallium nitride. The most comprehensive description of single crystal growth of gal-

lium nitride is given by Rabenau [6]. The largest single crystals described in the early literature appear to be ~5 mm and 10 to 30 μ m in diameter [7]. Two recent publications deal with epitaxial deposition of gallium nitride on single crystal substrates. The work of Maruska and Tietjen [2] describes the growth of colourless single crystal gallium nitride on sapphire substrates while Faulkner *et al* [8] report on the deposition of polycrystalline gallium nitride films on silicon carbide substrates. The present paper describes the preparation of colourless hexagonal single crystal needles of gallium nitride from a specially prepared powder. Raman scattering and infra-red absorption measurements have been made on these crystals and will be described in detail elsewhere [9]. The technique used for the synthesis of gallium nitride is an adaptation of the method of Johnson *et al* and is described below.

In a typical synthesis run, 5 to 6 g of 6-9's pure gallium are added to a clean BN boat.* The boat is then inserted into a BN* furnace liner and slowly heated in a stream of tank ammonia to ~1050°C. Gas flow rates are from 30 to 100 cc/min. The reaction begins at 1050°C and is allowed to continue overnight during which time the tube becomes partially blocked with

*Pyrolytic BN from Union Carbide Corporation.